

## Electronic Supporting Information (ESI)

### A photoinduced pH jump applied to drug release from cucurbit[7]uril

Cátia Parente Carvalho, Vanya D. Uzunova, José P. Da Silva,  
Werner M. Nau, Uwe Pischel\*

#### **1) General Remarks**

Hoechst 33258 trihydrochloride pentahydrate ( $\text{1H}_3^{3+}$ ; FluoroPure™ grade) was supplied by Invitrogen and used without further purification. Cucurbit[7]uril was synthesised according to a published procedure.<sup>1</sup> Malachite green leucohydroxide (MGOH, 90%) was from Aldrich. Water was of Millipore quality.

All UV/vis absorption and fluorescence measurements were done at ambient temperature (24 °C) in air-equilibrated aqueous solutions, using 1-cm quartz cuvettes. Absorption spectra were recorded on a UV-1603 spectrophotometer from Shimadzu. Steady-state fluorescence measurements were done on a Varian Cary Eclipse instrument. In the fluorescence titration experiments with CB7 an excitation wavelength of 295 nm was chosen. Generally, the dye concentration was kept low ( $\leq 10 \mu\text{M}$ ; in most cases  $1 \mu\text{M}$ ) to avoid aggregation.<sup>2</sup> The fluorescence lifetime measurements were performed at higher dye concentration (*ca.*  $100 \mu\text{M}$ ). The pH in the respective titrations was adjusted by addition of acid (HCl) or base (NaOH) and monitored during the course of the experiments. Where indicated, phosphate buffer (1 mM or 10 mM) was used. Fluorescence quantum yields were measured with quinine sulfate in 0.05 M  $\text{H}_2\text{SO}_4$  as a standard ( $\Phi_f = 0.55$ ).<sup>3</sup> The binding constants were obtained by fluorescence titrations of dye **1** with increasing amounts of CB7 at constant pH and fitted according to a 1:1 binding model.<sup>4</sup>

The mass spectrometric experiments were performed with a Bruker Daltonics HCT-Ultra mass spectrometer (ion trap), equipped with an electrospray ionisation (ESI) source (Agilent) that utilised a nickel-coated glass capillary with an inner diameter of 0.6 mm. Ions were continuously generated by infusing the aqueous solution samples into the source with a syringe pump (KdScientific, model 781100, USA) at flow rates of  $4 \mu\text{l}/\text{min}$ . The measurement parameters were adjusted and were typically as follows;

polarity: positive; capillary voltage:  $-4.0$  kV; capillary exit voltage:  $CE = 200$  V; skimmer voltage:  $25$  V; temperature of drying gas:  $300$  °C. The spectra were obtained in the “ultrascan mode” (fwhm  $0.6$  m/z). The experiments were done with a nebuliser gas pressure of  $30$  psi and a drying gas flow of  $8$  L/min. The measurements were carried out with mixtures of  $3$   $\mu\text{M}$  **1** and  $10$   $\mu\text{M}$  CB7 at pH  $4.5$ . Note that no significant 2:1 complexation is expected under these concentrations.<sup>5</sup>

<sup>1</sup>H-NMR spectra were recorded on an ECX400 spectrometer from JEOL. Solutions were prepared in D<sub>2</sub>O (99.9 atom% D) and if required their acidity was adjusted by addition of DCl stock solution (99 atom% D). The spectra are referenced to the HOD signal at  $4.67$  ppm.

For the pH jump experiments, solutions containing  $1$   $\mu\text{M}$  **1**,  $30$   $\mu\text{M}$  CB7, and  $100$   $\mu\text{M}$  MGOH were prepared at pH  $7.2$  (buffered or unbuffered). The MGOH was added in form of a few microliters of a  $100$  mM MGOH stock solution in dimethylsulfoxide. The thus prepared photolysis solution was allowed to equilibrate for *ca.*  $1.5$  hours in the dark, during which a small fraction ( $< 10\%$ ) of the MGOH converted thermally to  $\text{MG}^+$ . At the end of the equilibration the pH was measured and then the solution was irradiated for  $10$  minutes at  $300$  nm; the precise wavelength of the UVP hand-held lamp (model UVM-57) is  $302$  nm. Subsequently, the fluorescence spectrum was recorded ( $\lambda_{\text{exc}} = 340$  nm) and the pH was measured again. Finally, the solution was allowed to re-equilibrate in the dark and fluorescence spectra were recorded periodically and at the end of the procedure the pH was recorded once more.

## 2) Binding Constants

In the main text, the binding constant at pH 7.2 is given as  $(1.7 \pm 0.4) \times 10^6 \text{ M}^{-1}$ . This corresponds to the value fitted for the smallest employed dye concentration ( $0.2 \mu\text{M}$ , Fig. S1), which is preferable for high affinity binding. Fluorescence titrations at higher dye concentrations (Fig. S2 and S3), as well as a UV/vis titration (Fig. S4) afford systematically lower binding constants. In an independent study,<sup>5</sup> the binding constant at pH 7 has been reported as  $(1.45 \pm 0.1) \times 10^5 \text{ M}^{-1}$ . The fluorescence titration at pH 8.7 is shown in Fig. S5.

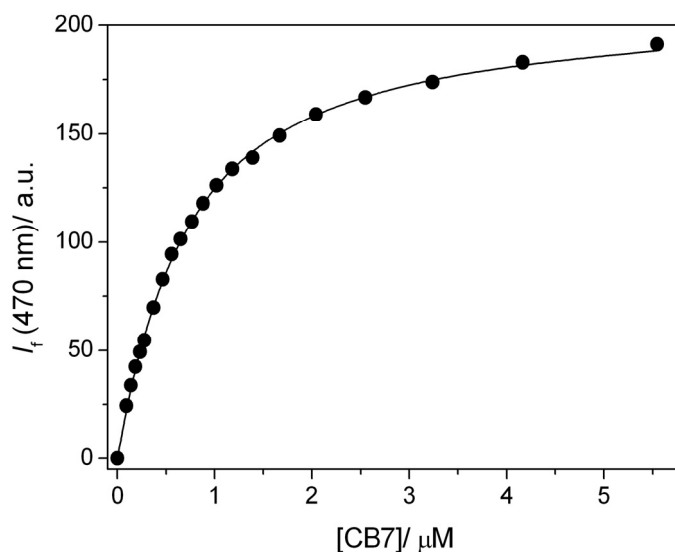


**Fig. S1** Fluorescence titration of  $0.2 \mu\text{M}$  **1** with CB7 at pH 7.2 (10 mM phosphate buffer). The effective binding constant was determined as  $K_b = (1.7 \pm 0.4) \times 10^6 \text{ M}^{-1}$ .

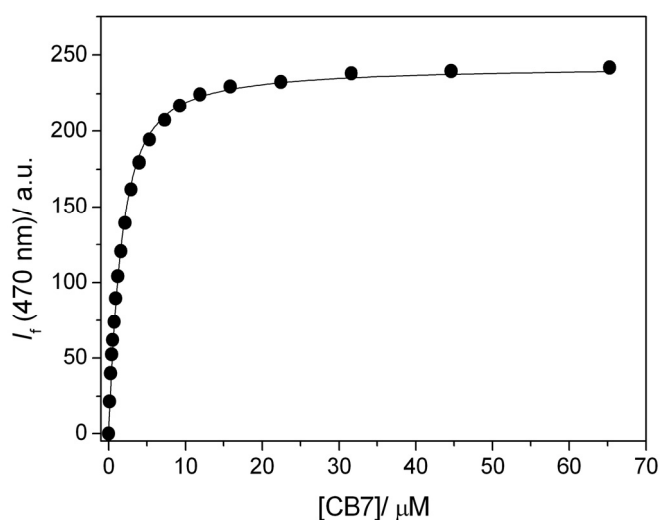


**Fig. S2** Fluorescence titration of  $1.2 \mu\text{M}$  **1** with CB7 at pH 7.2 (10 mM phosphate buffer). The effective binding constant was determined as  $K_b = (1.0 \pm 0.2) \times 10^6 \text{ M}^{-1}$ .

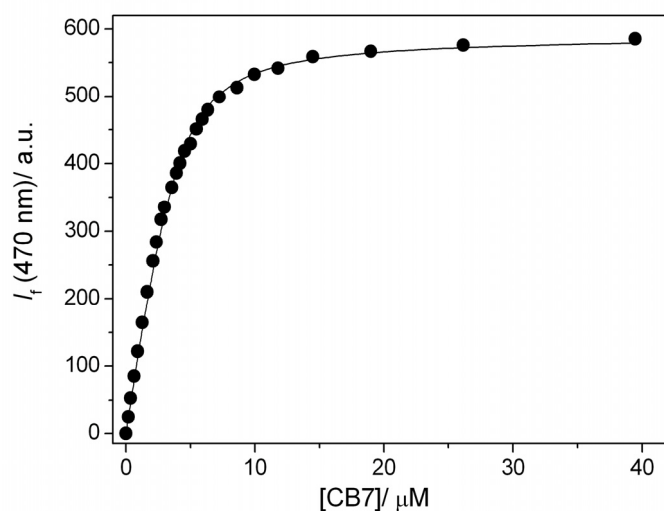


**Fig. S3** Fluorescence titration of 4  $\mu\text{M}$  **1** with CB7 at pH 7.2 (10 mM phosphate buffer). The effective binding constant was determined as  $K_b = (1.5 \pm 0.3) \times 10^6 \text{ M}^{-1}$ .

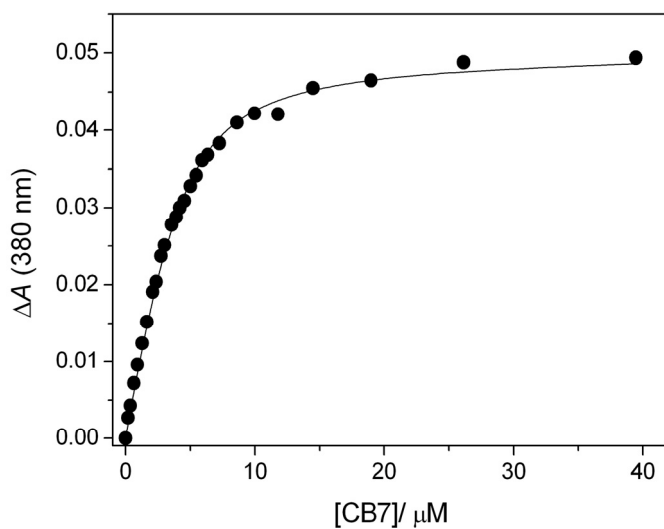


**Fig. S4** UV/vis absorption titration of 4  $\mu\text{M}$  **1** with CB7 at pH 7.2 (10 mM phosphate buffer). The effective binding constant was determined as  $K_b = (8.5 \pm 1.0) \times 10^5 \text{ M}^{-1}$ .

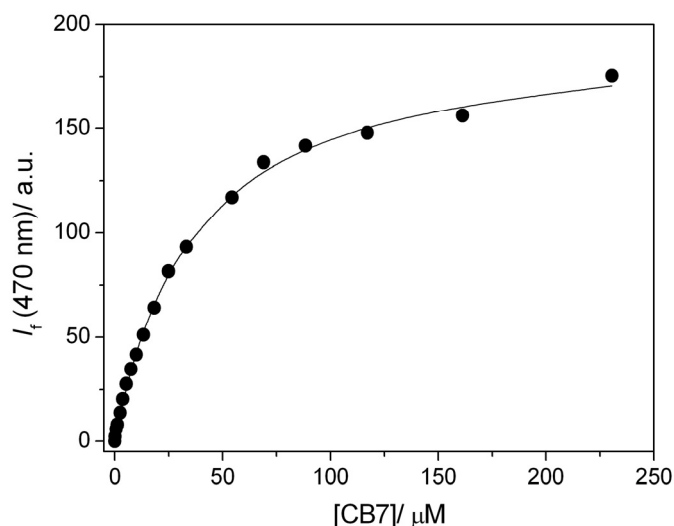


**Fig. S5** Titration of 1  $\mu\text{M}$  **1** with CB7 at pH 8.7 (10 mM phosphate buffer). The effective binding constant was determined as  $K_b = (2.8 \pm 0.2) \times 10^4 \text{ M}^{-1}$ .

### **3) Electrospray Ionisation Mass Spectrometry (ESI-MS)**

In order to gain deeper insight in the encapsulation of **1** by CB7, ESI-MS studies were performed. As shown in Fig. S6, different 1:1 complexes with two or three positive charges, containing  $\text{H}^+$  or  $\text{K}^+$ , were observed. MS/MS studies were used to assist the peak assignment (Fig. S7-S9). The fragmentation ( $\text{MS}^2$ ) of  $m/z$  794.5 ( $[\text{CB7} + \mathbf{1} + 2\text{H}]^{2+}$ ) gave  $m/z$  766.0 (Fig. S7), which corresponds to a still intact complex with a mass loss of 57. This mass loss was also observed for the fragmentation of the free guest (Fig. S10). Actually, such guest fragmentation inside a CB host under retention of the host-product complex has been recently precedented.<sup>6</sup> The strength of the complex is underlined by the failure to disassemble it into the guest and host components. As can be observed in Fig. S8, the situation was different for the fragmentation ( $\text{MS}^2$ ) of the ion corresponding to  $m/z$  813.4, which gave the free host ( $m/z$  1201.3,  $[\text{CB7} + \text{K}]^+$ ) and the free guest ( $m/z$  425.3,  $[\mathbf{1} + \text{H}]^+$ ). In addition, the ion corresponding to the fragmented free guest ( $m/z$  368.2,  $[\mathbf{1}(-57) + \text{H}]^+$ ), was observed. These results indicate that the  $m/z$  813.4 ion is the complex  $[\text{CB7} + \mathbf{1} + \text{H} + \text{K}]^{2+}$ . The fragmentation pattern of this ion hints on a less stable assembly as compared to  $m/z$  794.5. The ion at  $m/z$  530.0 was assigned to the triply charged species  $[\text{CB7} + \mathbf{1} + 3\text{H}]^{3+}$ . The fragmentation of this peak (Fig. S9) yielded  $m/z$  510.8 and 766.1, which correspond to a triply and doubly protonated complex, respectively, with the partially fragmented guest  $\mathbf{1}(-57)$  inside the CB7 macrocycle.

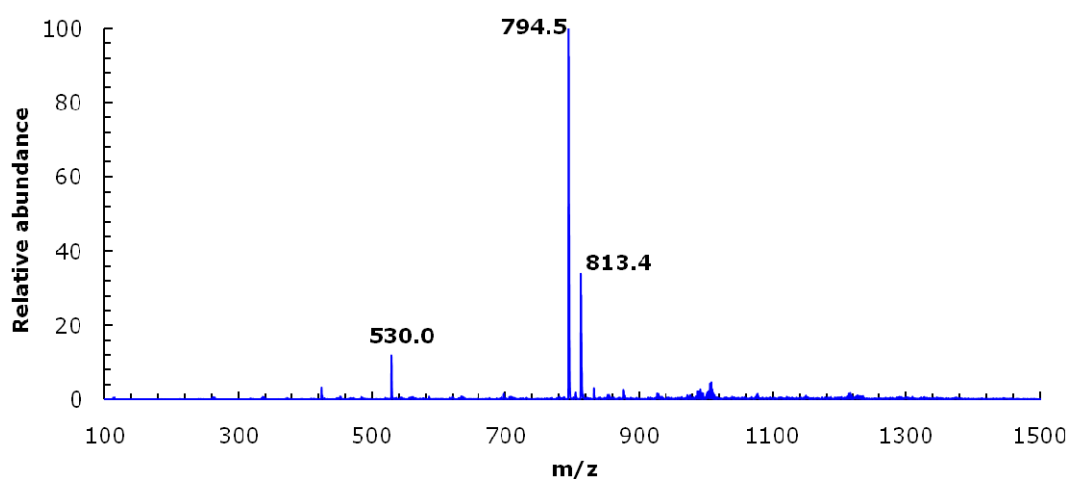


**Fig. S6** ESI-MS spectrum of the CB7·1 complexes at pH 4.5. Assignments:  $m/z$  530.0:  $[\text{CB7} + \mathbf{1} + 3\text{H}]^{3+}$ ; 794.5:  $[\text{CB7} + \mathbf{1} + 2\text{H}]^{2+}$ ; 813.4:  $[\text{CB7} + \mathbf{1} + \text{H} + \text{K}]^{2+}$ .

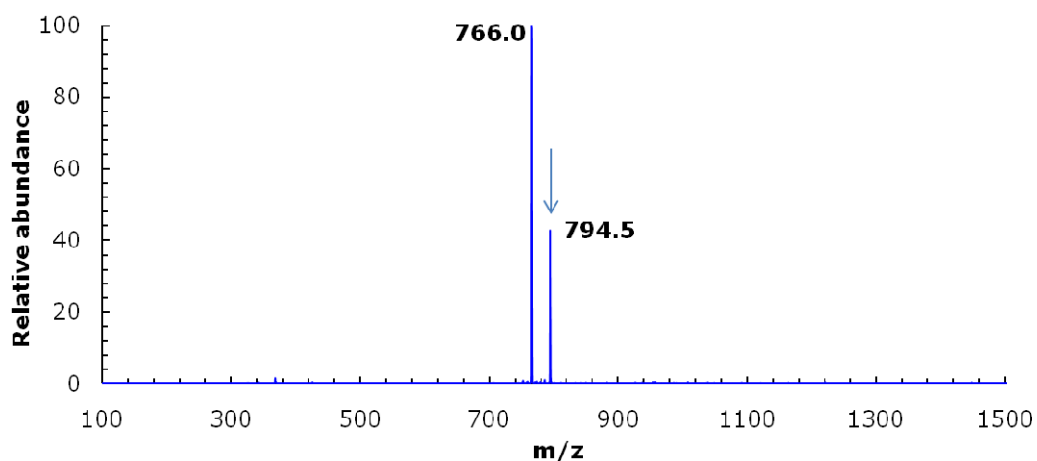


**Fig. S7** Fragmentation ( $\text{MS}^2$ ) of the  $m/z$  794.5 ion. The arrow indicates the fragmented ion. Assignments:  $m/z$  794.5:  $[\text{CB7} + \mathbf{1} + 2\text{H}]^{2+}$ ; 766.0:  $[\text{CB7} + \mathbf{1}(-57) + 2\text{H}]^{2+}$ .

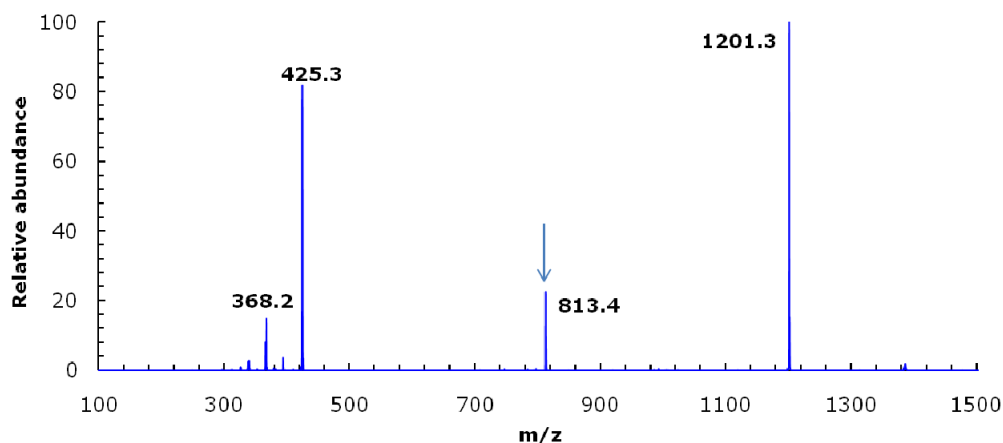


**Fig. S8** Fragmentation (MS<sup>2</sup>) of the  $m/z$  813.4 ion. The arrow indicates the fragmented ion. Assignments:  $m/z$  813.4: [CB7 + **1** + H + K]<sup>2+</sup>; 1201.3: [CB7 + K]<sup>+</sup>; 425.3: [**1** + H]<sup>+</sup>; 368.2: [**1**(-57) + H]<sup>+</sup>.

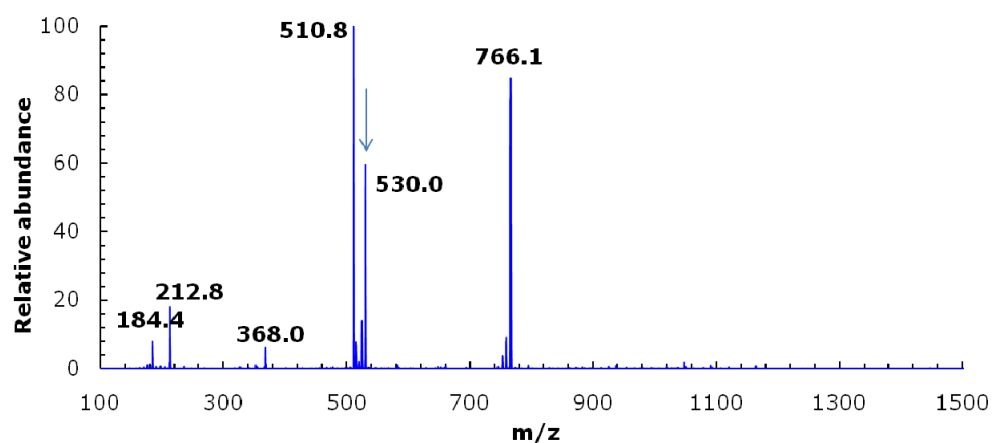


**Fig. S9** Fragmentation (MS<sup>2</sup>) of the  $m/z$  530.0 ion. The arrow indicates the fragmented ion. Assignments:  $m/z$  530.0: [CB7 + **1** + 3H]<sup>3+</sup>; 766.1: [CB7 + **1**(-57) + 2H]<sup>2+</sup>; 510.8: [CB7 + **1**(-57) + 3H]<sup>3+</sup>; 368.0: [**1**(-57) + H]<sup>+</sup>; 212.8: [**1** + 2H]<sup>2+</sup>; 184.4: [**1**(-57) + 2H]<sup>2+</sup>.

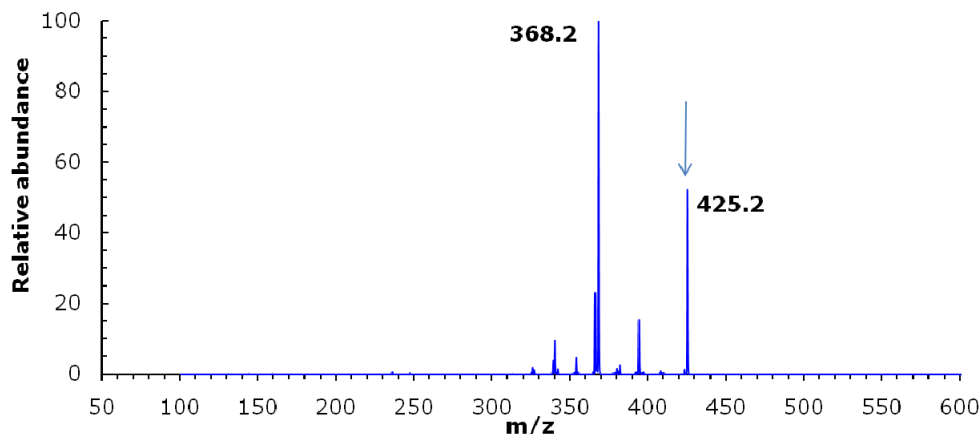


**Fig. S10** Fragmentation ( $MS^2$ ) of the  $m/z$  425.2 ion (free **1**, pH 7.0). The arrow indicates the fragmented ion. Assignments:  $m/z$  425.2:  $[1 + H]^+$ ; 368.2:  $[1(-57) + H]^+$ .

#### 4) $^1H$ NMR Spectra

The 1:1 stoichiometry of the CB7•**1** complex at pH 7 was confirmed by  $^1H$  NMR spectroscopy (Fig. S11). Typical upfield and downfield shifts of the dye peaks were observed upon addition of 1 eq. CB7 to the free dye **1**, which are indicative of host-guest complex formation. The addition of a second equivalent of CB7 led to practically no further signal shifts, which corroborates the formation of a 1:1 complex. Our results at neutral pH contrast the formation of 2:1 complexes in acidic solution (pH 4.5), as demonstrated in a recent study.<sup>5</sup>

For the determination of the binding mode of the dye in the 1:1 complex an acidic solution was preferred for  $^1H$  and 2D COSY NMR experiments, because the peaks of the free dye are better resolved under these conditions than at pH 7.<sup>7</sup> The formation of the 1:1 complex was assured by the addition of just 1 eq. CB7 to the dye. The peak assignments of **1** (Fig. S12 and S13) were done according to the literature.<sup>7</sup> Upon addition of 1 eq. CB7 to the guest, characteristic complexation-induced signal shifts were observed (Fig. S14). The proposed structure of the CB7•**1** complex rests on the general observation that upfield shifts correspond to protons immersed in the macrocyclic cavity (see also Fig. S15 for assignments). Furthermore, the complex shows fast exchange on the NMR time-scale accompanied by an apparent symmetry distortion of the CB7 methylene protons at *ca.* 5.5-5.6 ppm.

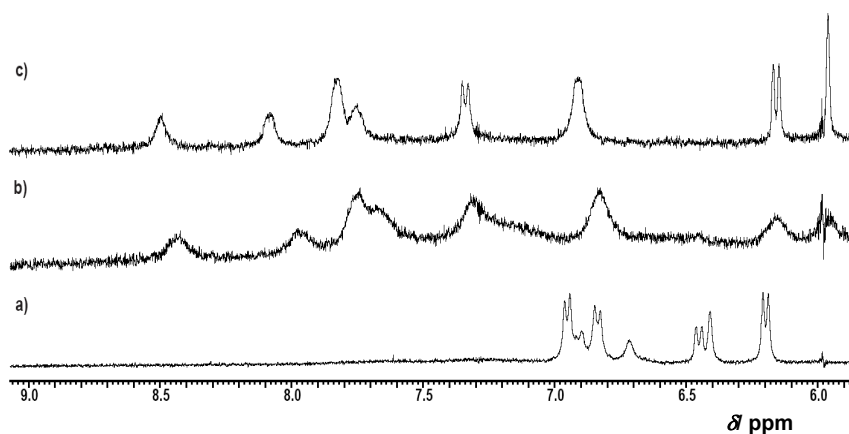


**Fig. S11**  $^1\text{H}$  NMR spectra at pH 7.0 of a) the free dye **1** (0.5 mM), b) **1** (0.5 mM) in the presence of 1 eq. CB7 (0.5 mM), and c) **1** (0.5 mM) in the presence of 2 eq. CB7 (1.0 mM).

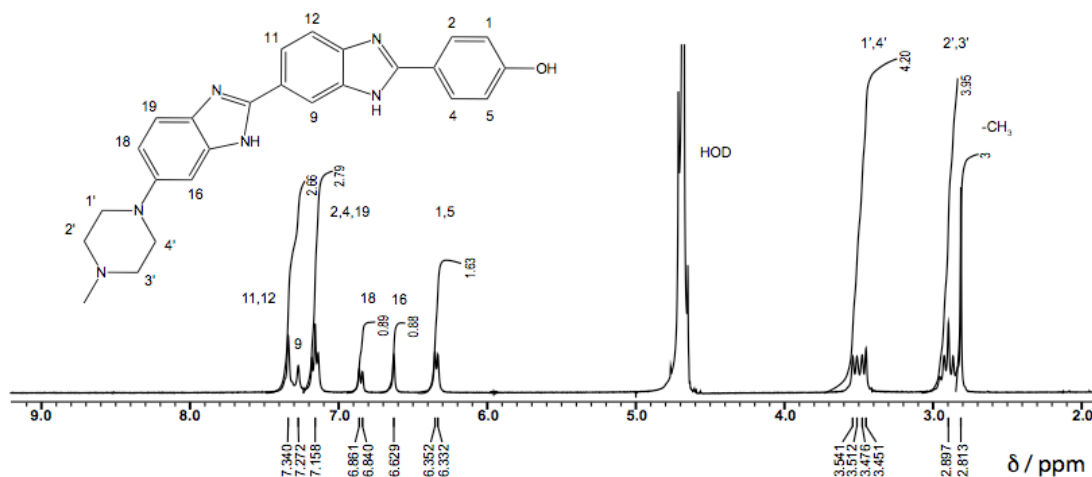


**Fig. S12**  $^1\text{H}$  NMR spectrum of **1** (5 mM) in 50 mM DCl. Peak assignments were made according to ref.<sup>7</sup> and the COSY spectrum (see Fig. S13).

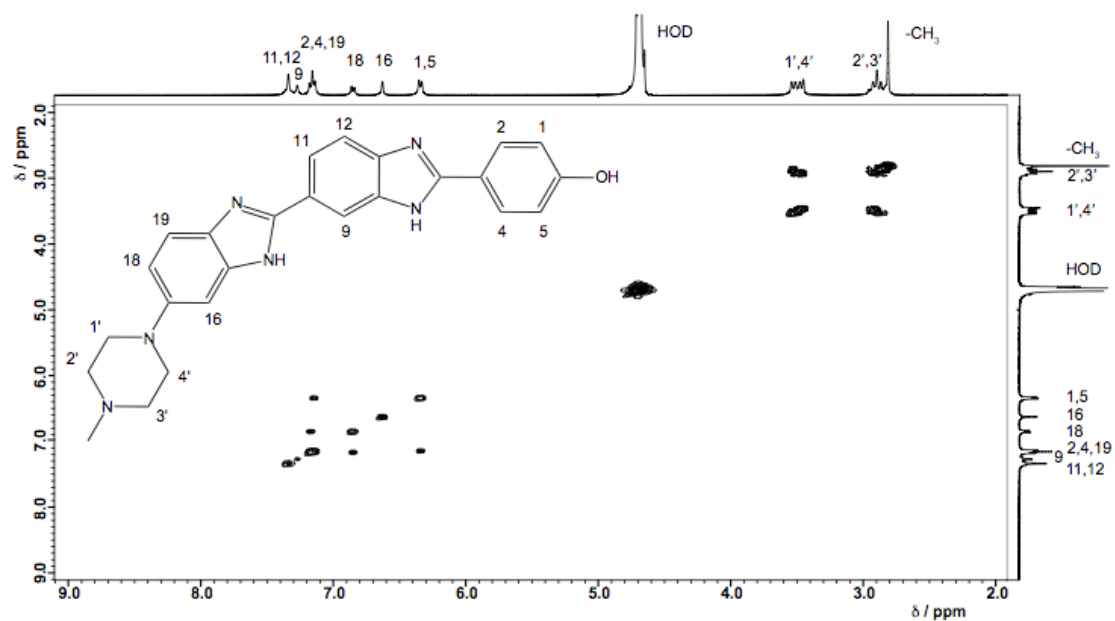


**Fig. S13** COSY spectrum of **1** (5 mM) in 50 mM DCl.

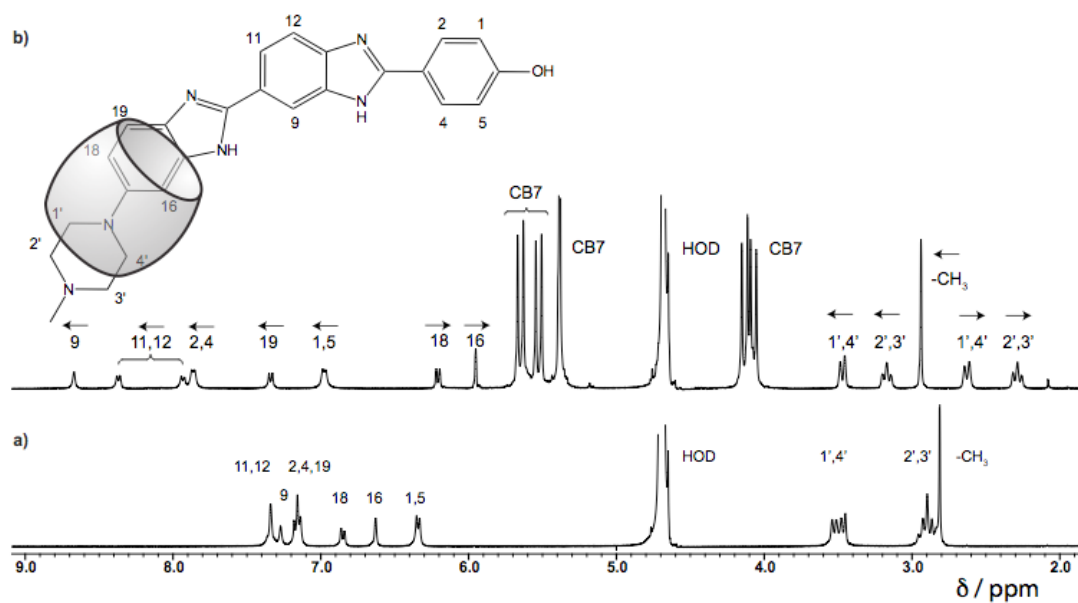


**Fig. S14** Comparison of the  $^1\text{H}$  NMR spectra of a) **1** (5 mM) in its free form in 50 mM DCl and b) **1** (3 mM) in the presence of CB7 (3 mM) in 10 mM DCl. Characteristic complexation-induced shifts are highlighted with arrows. In the proposed structure of the complex, the CB7 macrocycle is represented as a barrel.

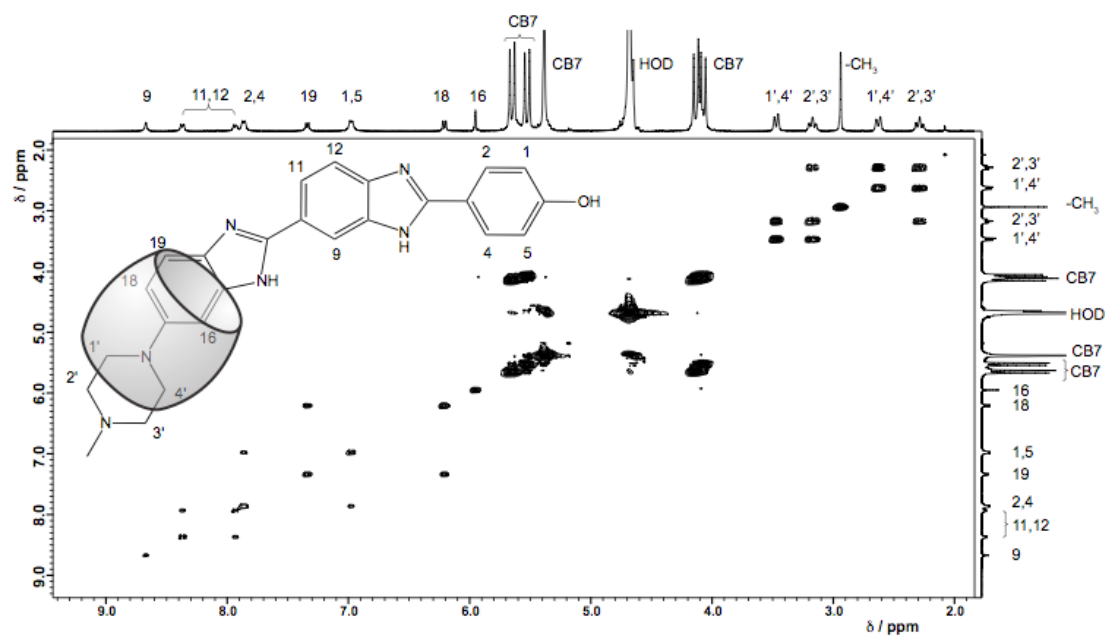


**Fig. S15** COSY spectrum of **1** (3 mM) in the presence of CB7 (3 mM) in 10 mM DCl.

### **5) Job's Plot Analysis**

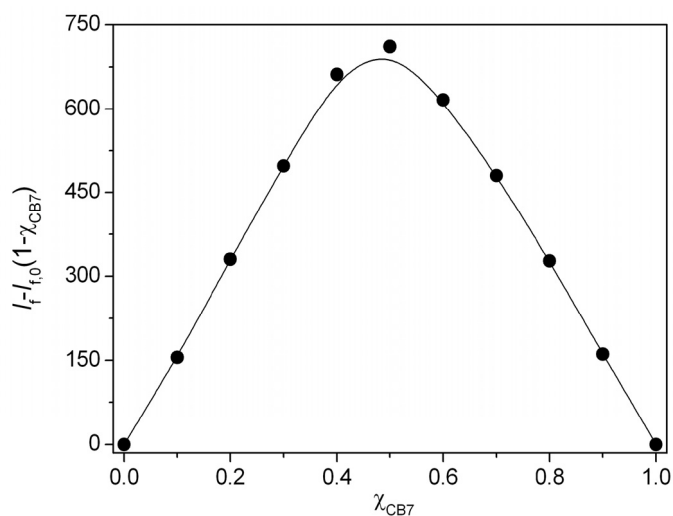


**Fig. S16** Job's plot for binding of **1** by CB7 at pH 7 (1 mM phosphate buffer). The formation of a 1:1 complex is evidenced by the maximum at 0.5.

### **6) 1:1 versus 2:1 Complex Formation**

Recently, the formation of a 2:1 CB7•**1** complex has been discussed.<sup>5</sup> However, under our experimental conditions above pH 7 we found no conclusive evidence for the involvement of such higher-order complexes. The 1:1 complexation stoichiometry has been unambiguously confirmed by Job's plot analysis in 1 mM phosphate buffer (Fig. S16), and supported by the ESI mass spectrometry studies (Fig. S6-S9). The fitting of the binding curves according to a 1:1 complexation model articulated the same stoichiometry (Fig. S1-S5). Finally, <sup>1</sup>H NMR studies (Fig. S11) revealed only very small shift changes for the presence of more than 1 eq. CB7. In addition, the complexation of a second CB7 would be expected to lead to the host inclusion of the phenol-substituted benzimidazole unit. However, the absence of (for the complexation highly characteristic) upfield shifts for the corresponding protons speaks against higher-order complexes under our experimental conditions. This does not exclude the existence of such species, especially in more acidic solutions (pH 4.5).<sup>5</sup>

## 7) Competitive Complexation of $\text{MG}^+$

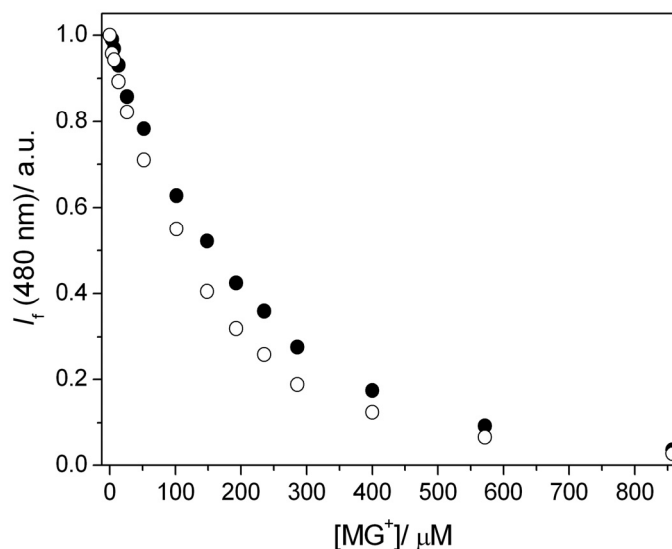


**Fig. S17** Titration of **1** ( $1 \mu\text{M}$ ) with malachite green cation ( $\text{MG}^+$ ) in the absence (empty circles) and presence (filled circles) of CB7 ( $30 \mu\text{M}$ ) at pH 4.5; emission was monitored at  $\lambda_{\text{obs}} = 480 \text{ nm}$ . At the chosen pH,  $\text{MG}^+$  is thermally sufficiently stable to carry out the experiment. The similarity of both curves excludes significant competitive binding. At much higher concentrations of the cation than those generated under the photolysis conditions (*ca.*  $20 \mu\text{M}$   $\text{MG}^+$ ), inner filter effects become experimentally significant. The weak competition of  $\text{MG}^+$  with **1** is in agreement with the rather low binding constant of the closely related brilliant green cation with CB7 ( $K_b = 1.7 \times 10^4 \text{ M}^{-1}$ ).<sup>8</sup> The contribution of competitive binding of  $\text{MG}^+$  to the observed fluorescence decrease (see Fig. 3 in main text) must be minor in any case, since the control experiment in buffered solution (in which  $\text{MG}^+$  is formed with the same efficiency) does not produce a sizeable fluorescence response (inset of Fig. 3 of main text).

## 8) Photolysis of MGOH

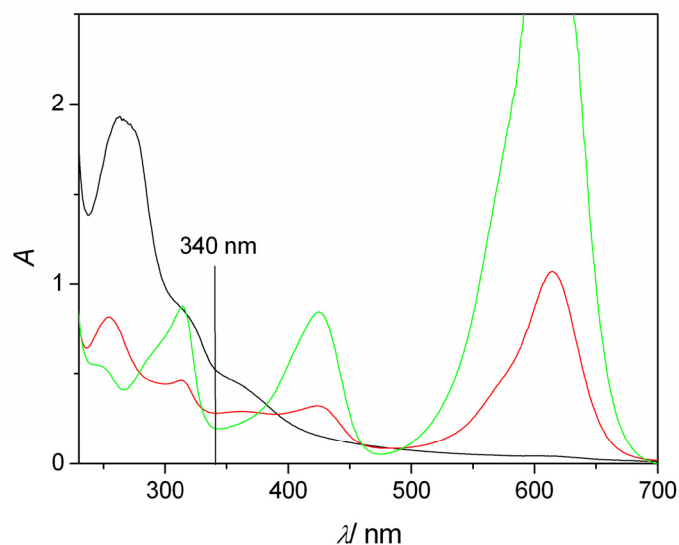


**Fig. S18** UV/vis absorption spectra of the solution containing 1  $\mu\text{M}$  **1**, 30  $\mu\text{M}$  CB7, and 100  $\mu\text{M}$  MGOH: a) immediately after addition of MGOH (black line), b) after equilibration for *ca.* 1.5 hours (red line), and c) after photolysis with UV light for 10 minutes (green line). *Ca.* 20  $\mu\text{M}$  MGOH are converted to  $\text{MG}^+$  under these conditions; estimated from its nascent absorption band.

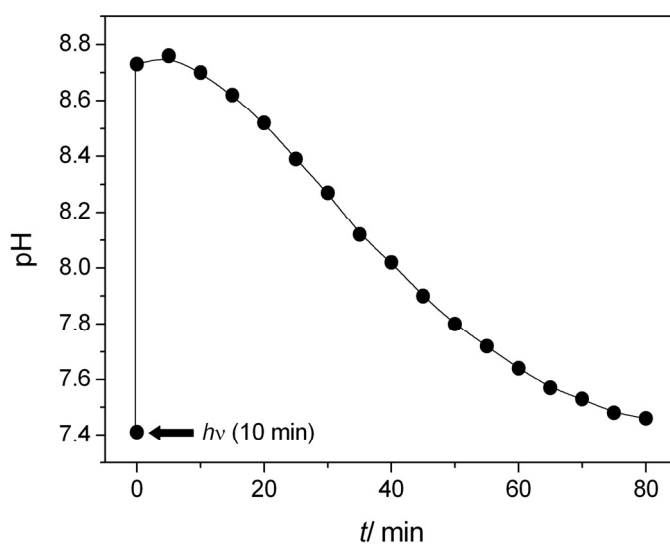


**Fig. S19** Temporal development of pH after photoinduced pH jump of a solution containing 1  $\mu\text{M}$  **1**, 30  $\mu\text{M}$  CB7, and 100  $\mu\text{M}$  MGOH.

## References

1. C. Márquez, F. Huang and W. M. Nau, *IEEE Trans. Nanobiosci.*, 2004, **3**, 39.
2. H. Görner, *Photochem. Photobiol.*, 2001, **73**, 339.
3. J. V. Morris, M. A. Mahaney and J. R. Huber, *J. Phys. Chem.*, 1976, **80**, 969.
4. H. Bakirci and W. M. Nau, *Adv. Funct. Mater.*, 2006, **16**, 237.
5. N. Barooah, J. Mohanty, H. Pal and A. C. Bhasikuttan, *Phys. Chem. Chem. Phys.*, 2011, DOI: 10.1039/C1CP20493A.
6. N. Saleh, M. Meetani, L. Al-Kaabi, I. Ghosh and W. M. Nau, *Supramol. Chem.*, 2011, 10.1080/10610278.2011.593631.
7. J. A. Parkinson, J. Barber, B. A. Buckingham, K. T. Douglas and G. A. Morris, *Magn. Reson. Chem.*, 1992, **30**, 1064.
8. A. C. Bhasikuttan, J. Mohanty, W. M. Nau and H. Pal, *Angew. Chem., Int. Ed.*, 2007, **46**, 4120.